Optik 125 (2014) 3102–3106

Contents lists available at ScienceDirect

Optik

journal homepage: www.elsevier.de/ijleo

Pose estimation for UAV aerial refueling with serious turbulences based on extended Kalman filter

Yan Xu [a], Delin Luo [a,b], Ning Xian [a], Haibin Duan [a,*]

[a] State Key Laboratory of Virtual Reality Technology and Systems, Beihang University, Beijing 100191, PR China
[b] School of Information Science and Technology, Xiamen University, Xiamen 361005, PR China

ARTICLE INFO

Article history:
Received 21 June 2013
Accepted 15 December 2013

Keywords:
Unmanned aerial vehicle (UAV)
Aerial refueling
Machine vision
Pose estimation
Extend Kalman filter

ABSTRACT

In recent years, many pose estimation algorithms were developed, and have been successfully applied to solve unmanned aerial vehicle (UAV) aerial refueling pose estimation problems. This paper mainly focuses on solving this problem under serious turbulences circumstance. The extended Kalman filter is a set of mathematical equations to estimate the state of a process, which is able to support estimations of past, present, and even future states. In reference to previous papers and some simulations, we build up the noise models of refueling boom and atmospheric turbulence. Then, an extend Kalman filter is adopted to solve the pose estimation problem in UAV aerial refueling with serious turbulences. The experimental results demonstrate the feasibility and effectiveness of our proposed approach.

1. Introduction

Unmanned aerial vehicles (UAVs) play an increasingly important role in military actions in the information age. However, the research on UAV's aerial refueling is in an initial state, which in turn causes a bottleneck of its performance [1]. Aerial refueling enables UAVs to travel anywhere if needed by extending their durance and range, which will greatly increase the UAV's fighting radius and airborne period. UAV's aerial refueling is an essential part to update its performance [2]. By measuring the image sequence, it can obtain one flight's navigation parameters, such as speed, altitude, and flying direction, which are essential for providing navigation information [3–7].

Aircraft visual navigation is a new rapidly developed international navigation technology in the past two decades [8]. By using a visible light or an infrared camera installed on one vehicle, it is possible to identify a target such as radar on the ground or another flight vehicle [9,10]. The estimation of the 3D orientation and the position of an object from its images is called 'pose estimation' in the computer vision research community [11]. The modeling of an aircraft has been continuously investigated for many years, and several nonlinear aircraft models of UAV and tanker have been developed using the conventional modeling procedures [12,13].

In 1960, R.E. Kalman described a recursive solution to the discrete-data linear filtering problem. The Kalman filter is a set of mathematical equations that provides an efficient computational (recursive) means to estimate the state of a process, in a way that minimizes the mean of the squared error [14]. Since the measurement and estimation process is not linear in this situation, an extended Kalman filter is introduced to solve this problem. This work tried to solve the aerial refueling pose estimation problems by using extended Kalman filter, and experimental results are also given for verifying the feasibility of this scheme.

2. The modeling of aircraft boom and turbulence

2.1. Model of the aircraft

The nonlinear models of the UAV and the tanker have been developed via flight gear software. Through this software, we choose the "KC-135" model for the tanker, while the F-16 model is a similar nonlinear model for the modeling of the UAV. Then a conventional state vector is can be demonstrated like:

$$F = [v, x, y, \psi, \theta, \varphi] \tag{1}$$

where V denotes the aircraft velocity, x, y, z represent the position in the earth reference frame, ψ, θ, φ are the components of the angular velocity in the body reference frame, which denotes pitch, yaw and, roll angle, respectively.

2.2. Model of the aerial refueling

To describe the aerial refueling problem, it is necessary to define several reference frames (RFs), that is:

* Corresponding author. Tel.: +86 10 8231 7318.
E-mail address: hbduan@buaa.edu.cn (H. Duan).

0030-4026/$ – see front matter © 2014 Elsevier GmbH. All rights reserved.
http://dx.doi.org/10.1016/j.ijleo.2014.01.014

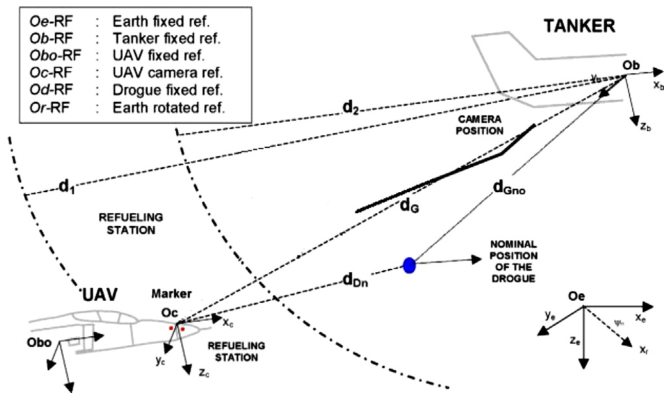

Fig. 1. Reference frames and notation.

(1) Oe-RF or E: earth-fixed reference frame.
(2) Obo-RF or U: the body-fixed UAV reference frame.
(3) Ob-RF or T: the body-fixed tanker reference frame.
(4) Oc-RF or C: the body-fixed UAV camera reference frame.

For indicating points, we use homogeneous coordinates. For instance, a point P indicated in the E reference frame will be demonstrated as ${}^{E}P=[x, y, z, 1]^T$, in which the superscript 'T' on the right side is for the transposition of the matrix.

To indicate the distance of two points, we define two capital letters with a left superscript indicating the reference frame. For instance, ^{C}MN represents a distance vector from point M to point N in the camera reference frame.

In some situations, the points and vectors should be transformed from the initial reference frame to another one, whose transformation matrix can be denoted as T with a right subscript representing the initial reference frame and a left subscript representing the ultimate frame. For example, ${}^{T}T_C$ represents the transformation matrix that transforms points or vectors from the Ob-RF to the Oc-RF. Fig. 1 shows the related reference frames [4].

2.3. Modeling of the boom

Recently, a detailed model of the boom has been developed for simulation. The mathematical model of the boom can be defined using Lagrange method [15]:

$$\frac{\mathrm{d}}{\mathrm{d}x}\frac{\partial L(q,\dot{q})}{\partial \dot{q}_i} - \frac{\partial L(q,\dot{q})}{\partial q_i} = F_i, i =, \ldots, n \qquad (2)$$

where $L(q, \dot{q}) = T(q, \dot{q}) - U(q)$ is the Lagrangian. Q defines the position and orientation of the boom. F_i represents some wind and control forces, which affects the boom.

The boom can be demonstrated in the tanker reference frame with x, y, z. The boom is telescopic so it is able to extend itself or pull it back, for which we use a d to describe. Installed on few wings, it has the ability to do vertical and lateral relative rotations which is θ, φ. Thus, the boom has 6 degrees of freedom described as $P=(x, y, z, \theta, \varphi, d)$.

2.4. Modeling of the turbulence

The research about the turbulence has also been developed for a long time. Birhle applied research lab in the Langley full scale tunnel [16,17] conducted several experiments about KC-135 in simulation environment. By testing the amplitude from the boom swinging, they drew pictures about the trajectory of vertical and lateral directions.

Through the Simulink, we utilize these data to build a block, which can continuously provide perturbations for the 6 aerodynamic coefficients. Then, all of these models are considered in the pose estimation progress.

3. Image processing on the aerial refueling

3.1. The process on the image

As mentioned above, the UAV model now has been built. The red color of the receptacle on the UAV can be used as characteristic information for feature extraction. The camera on the tanker is installed nearby the boom. Once the picture has been obtained, the machine vision (MV) [18] based system transforms the image from RGB space to the HSV space. Then we convert the captured image into a binary one by setting threshold of the color.

3.2. The threshold segmentation in HSV color space

The HSV space is created base on the intuitive colors, which is appropriate for human vision sense. The HSV space can be described as an inverted hexagonal pyramid, hue (H) indicates different colors, saturation (S) represents the color depth, and the light and shade is represented with value (V).

In this work, the target's color is demonstrated as $S=0.9$, so we set a threshold of the picture. Through this progress, the target color will forcibly be changed into white while other colors will be changed into black.

The process of one point from RGB space to HSV space is based on the following formula:

$$\begin{cases} V = \dfrac{1}{3}(R+G+B) \\ S = 1 - \dfrac{3}{(R+G+B)}(\min(R, G, B)) \\ H = \arccos\left\{\dfrac{[(R-G)+(R-B)]/2}{\sqrt{[(R-G)^2+(R-B)(G-B)]}}\right\} \end{cases} \qquad (3)$$

3.3. Erosion to denoising

In image processing, erosion is denoted as Θ, if A is eroded by B, it can be described as:

$$A\Theta B = \{x|(B)_x \subseteq A\} \qquad (4)$$

Once the image has been segmented, there may still exist a few points with similar colors, which will cause a few noises to affect the results. By further processing with erosion method, the white area on the image would be shrunk, thus the noise points could be filtered.

3.4. Simulation results

The model has been built in flight gear and through the Simulink we added in it some modules of control and turbulence. The camera on the tanker captures a picture shown in the left of Fig. 2. Through the image processing part, the MV-system makes a segment of the picture. At last, the picture is dealt with an erosion part. The results are given in Fig. 2.

Through the feature extraction part, we can get the number of the points and each point's pixel in the pixel ordinates. The picture is 640×480 size. Based on the progress above, we can obtain all the data needed, which are listed in Table 1.

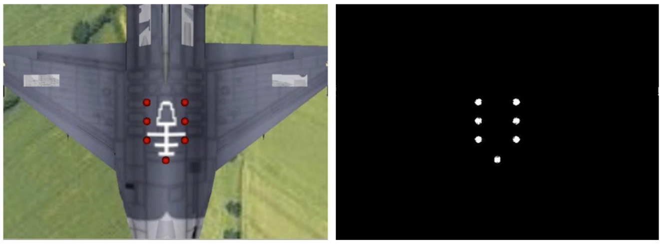

Fig. 2. The origin image and its result from image processing.

Table 1
The Feature Points And Their Pixel.

Point	Pixel(x)	Pixel(*y*)
1	235.0	288.6
2	197.2	288.8
3	273.0	288.8
4	314.1	327.1
5	197.2	365.4
6	234.8	365.3
7	273.2	365.8

4. The pose estimation algorithm

4.1. Pose estimation in aerial refueling

Following the solution of the image processing, the information in the set of points must be used to derive the rigid transformation from the camera reference frame to the UAV body reference frame [19].

Pose estimation is the conversion between two reference frames which can be described as a rotation matrix R and a transformation vector T shown in Fig. 3. If we know the coordinates of those feature points in the UAV body reference frame and their coordinates in the pixel reference frame, we can use R and T to describe their relationship. Once R and T are obtained, the position and orientation between UAV and tanker could be recognized.

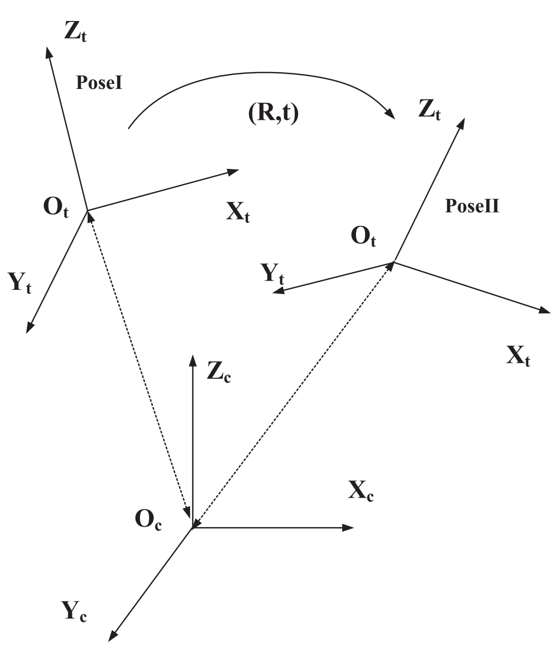

Fig. 3. Conversion between two reference frames.

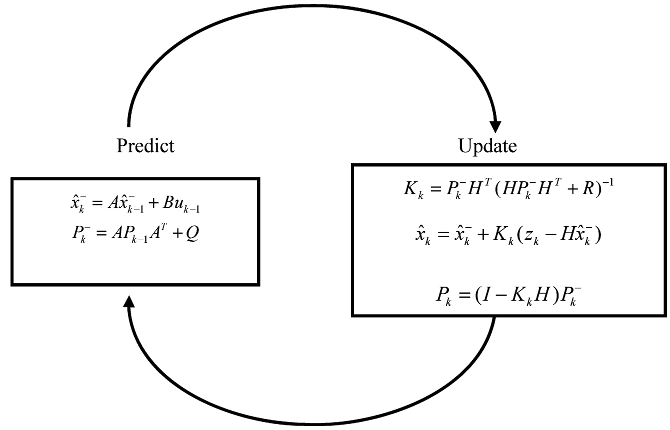

Fig. 4. Typical Kalman filter progress.

4.2. The Kalman filter

In 1960, R.E. Kalman described a recursive solution to the discrete-data linear filtering problem. The Kalman filter is a set of mathematical equations that provides an efficient computational (recursive) means to estimate the state of a process, in a way that minimizes the mean of the squared error [20].

The Kalman filter tries to estimate the state $x \in R^n$ of a discrete-time controlled process that is governed by the linear stochastic difference equation:

$$X(k) = \mathrm{Ax}(k-1) + \mathrm{Bu}(k-1) + w(k-1) \tag{5}$$

With a measurement $z \in R^{\mathrm{m}}$:

$$z(k) = \mathrm{Hx}(k) + v(k) \tag{6}$$

where $w\ (k)$ and $v\ (k)$ represent the process and measurement noises respectively, which are assumed to be independent with each other. Normally, these noises are set up with the following standard Gaussian noises.

$$p(w) \sim N(0, Q) \tag{7}$$

$$p(v) \sim N(0,\ R) \tag{8}$$

In practice, the process noise covariance and measurement noise covariance matrices might change with each time step or measurement, however, here we assume they are constants [21]. The whole estimation progress can be separated into two parts. One is 'predict' and the other is 'update'. This process can be shown in Fig. 4.

4.3. Extended Kalman filter

Since the measurement and estimation process is nonlinear in this situation, a Kalman filter that linearizes about the current mean and covariance is referred to as an extended Kalman filter (EKF) [22].Therefore, the process is now organized as a formulation:

$$X(k) = f(x(k-1), u(k-1), w(k-1) \tag{9}$$

While a measurement $z \in R^{\mathrm{m}}$:

$$z(k) = H(x(k), v(k)) \tag{10}$$

To estimate the following rotation angle with a motion model, the motion model should maintain the current angle value and angular velocity. The angle value and angular velocity are described by the linear state space:

$$x(k) = \begin{bmatrix} x & \dot{x} \end{bmatrix}^T \tag{11}$$

where $\dot{x}$ is the angular velocity. Assume that between the (k-1)-th and k-th time steps, the system undergoes a constant angular

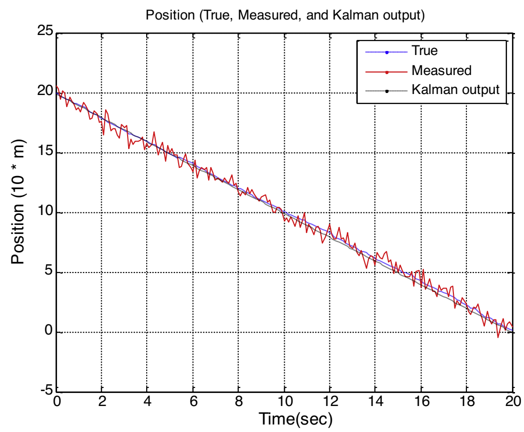

Fig. 5. The true, measured and Kalman output trajectory.

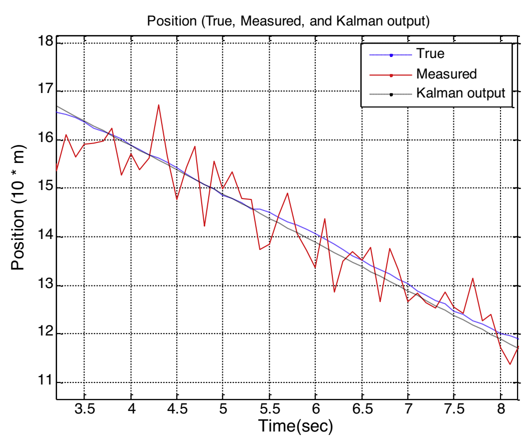

Fig. 6. The zoomed results of Fig. 5.

acceleration of $a(k)$, which is normally distributed with zero mean through Δt time interval.

In this work, we first linearize the measurement and process function by calculating their Jacobi matrix. Then we set up the measurement and process noise according to the model summarized in Section 3. Additionally, the initial state of the UAV $X(0)$ and the initial covariance $P(0)$ are also should be set with a definite value. Then we can estimate the pose by repeating the 'predict' and 'update' procedure.

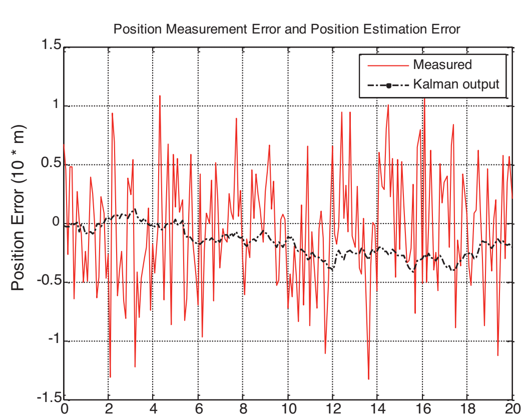

Fig. 7. The position error between the measured and Kalman output.

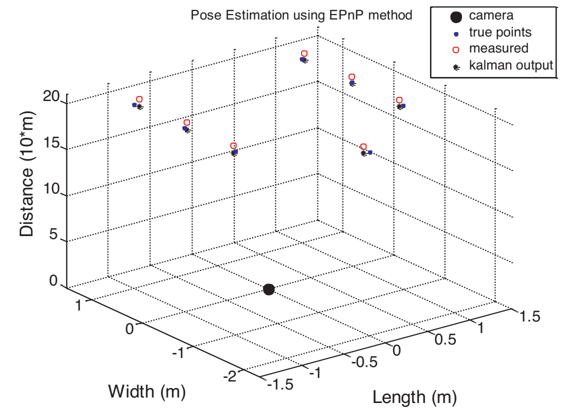

Fig. 8. $t = 0$ s each point pose in 3D world reference frame.

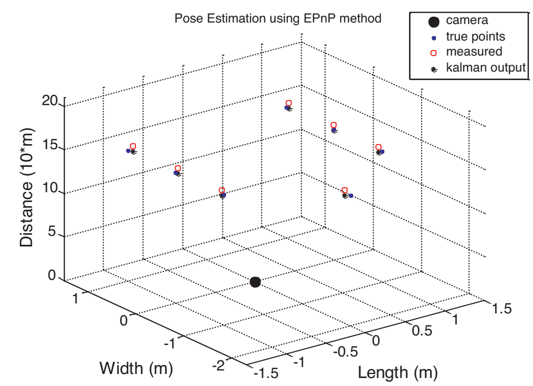

Fig. 9. $t = 5$ s each point pose in 3D world reference frame.

5. Experimental results and analysis

A series of simulation experiments are conducted in the developed aerial refueling environment. Since the extended Kalman filter is an iterative algorithm, which is based on a series data. Moreover, this step of estimation is affected by the previous estimation and will have influence on the next step.

According to this situation, we focus on this circumstance: assume the UAV can be recognized constantly by the camera nearby the refueling boom. The two flights will exchange any relative data to help maintain the refueling progress. The MV-based system can analyze the image and be able to successfully extract the feature points. Once this image processing is completed, this system will then start the pose estimation procedure to identify the position

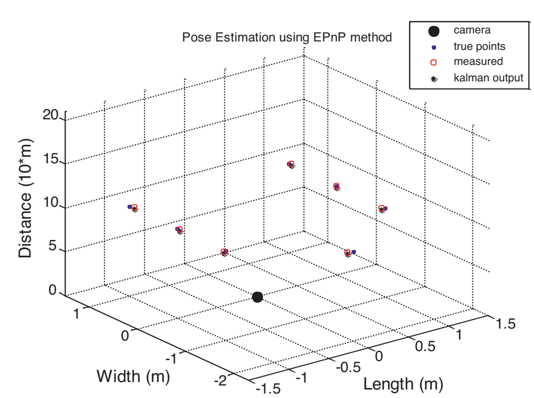

Fig. 10. $t = 10$ s each point pose in 3D world reference frame.

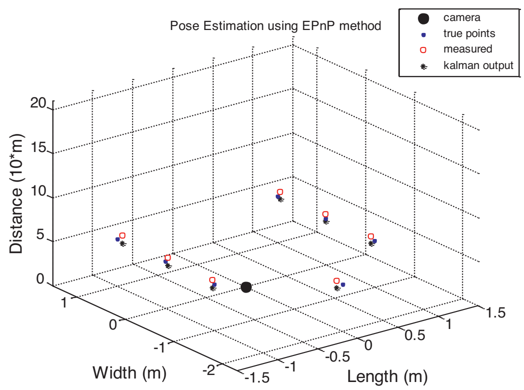

Fig. 11. $t = 15$ s each point pose in 3D world reference frame.

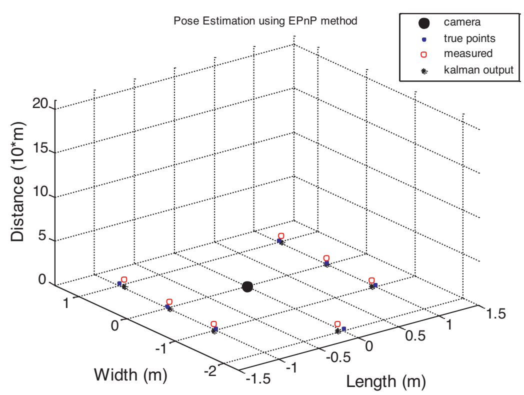

Fig. 12. $t = 20$ s each point pose in 3D world reference frame.

and orientation between the two flights. Then UAV can make a close-loop control to accomplish the whole mission.

In our simulation environment, it is assumed that the UAV and the tanker are set at the beginning. Then the UAV starts to approach the refueling boom. For simplification, the control law is approximately a uniform linear motion. However, the real control law remains being unknown. This work tried to estimate at each sample time using the extended Kalman filter. The simulation time is 20 s while the sample time is 0.1 s. The results are given in Fig. 5.

However, the result is optimized through the extended Kalman filter. For recognizing conveniently, we zoom in this figure and show part of this result (See Fig. 6).

Compared the measured position error with the Kalman output one, Fig. 7 shows the detailed result.

Through applying the extended Kalman filter, the obtained pose is more accurate than the measured one. Therefore, we can see that this method is effective in solving the pose estimation problem.

In the 3D world reference frame, this work picks out 5 states from the whole process, which are shown in Figs. 8–12.

From the series of experimental results, it is obvious that the measured error is random due to all the turbulences. By using extended Kalman filter, the results are more accurate in the whole process. The results show that this presented method can successfully solve the pose estimation problem for UAV aerial refuling in turbulence situation.

6. Conclusions

In this paper, we aim to solve the UAV aerial refueling problem in turbulence circumstance. First, we build the model of the aircraft, boom and turbulence according to previous results and our simulation which can represent the real world situation. Then, we utilize one feature extraction algorithm to extract relative feature points. As a result, the color points we set before can be recognized correctly and their coordinates should also be known. Finally, we introduce the extend Kalman filter to achieve the pose estimation procedure, whose model is established on the former two charters. Through simulation, this method is proved to be able to successfully solve this problem with high accuracy.

Acknowledgements

This work was partially supported by National Key Basic Research Program of China (973 Project) under grant #2013CB035503, National Magnetic Confinement Fusion Research Program of Chinaunder grant #2012GB102006, and Aeronautical Foundation of China under grant #20135851042 and 20115868009, and Open Funding Project of State Key Laboratory of Virtual Reality Technology of and Systems under grant # BUAA-VR-13KF-01.

References

[1] J.P. Nalepka, J.L. Hinchman, Automated aerial refueling: extending the effectiveness of unmanned air vehicles, in: AIAA Modeling and Simulation Technologies Conference and Exhibit, August 2005, San Francisco, California, 2005, pp. 15–18.
[2] Z. Jin, T. Shima, C.J. Schumacher, Optimal scheduling for refueling multiple autonomous aerial vehicles, IEEE Trans. Robot. 22 (4) (2006) 682–693.
[3] H. Duan, Y. Deng, X. Wang, F. Liu, Biologically eagle-eye visual imaging guidance simulation platform for unmanned flying vehicle, IEEE Aerosp. Electron. Syst. Mag. 28 (11) (2013) 36–45.
[4] H. Duan, Q. Zhang, Artificial bee colony algorithm with chaotic-search strategy approach to target recognition in UAV automatic landing, AIAA J. Aerosp. Comput. Inform. Commun. (2013), in press.
[5] Y. Deng, H. Duan, Biological edge detection for UCAV via improved artificial bee colony and visual attention, Aircr. Eng. Aerosp. Technol. 86 (2) (2013), in press.
[6] H. Duan, Q. Luo, Y. Yu, Trophallaxis network control approach to formation flight of multiple unmanned aerial vehicles, Sci. China Technol. Sci. 56 (5) (2013) 1066–1074.
[7] H. Duan, S. Liu, Nonlinear dual-mode receding horizon control for multiple UAVs formation flight based on chaotic particle swarm optimization, IET Control Theory Appl. 4 (11) (2010) 2565–2578.
[8] P. Li, H. Duan, Path planning of unmanned aerial vehicle based on improved gravitational search algorithm, Sci. China Technol. Sci. 55 (10) (2012) 2712–2719.
[9] R.M. Haralick, C.-N. Lee, Analysis and solutions of the three point perspective pose estimation problem, in: IEEE Computer Society Conference on Computer Vision and Pattern Recognition, Maui, Hawaii, 1991, pp. 592–598.
[10] C.-P. Lu, G.D. Hager, E. Mjolsness, Fast and globally convergent pose estimation from video images, IEEE Trans. Pattern Anal. Machine Intell. 22 (6) (2000) 610–622.
[11] B.K.P. Horn, H.M. Hilden, S. Negahdaripour, Closed-form solution of absolute orientation using orthonormal matrices, J. Opt. Soc. Am. A 5 (7) (1988) 1127–1135.
[12] E. Bernard, Dynamics of Atmospheric Flight, Dover Publications Inc., New York, 2005.
[13] M.O. Rauw, A Simulink Toolbox for Flight Dynamics and Control Analysis, Zeist, The Netherlands, 1997.
[14] G. Bishop, G. Welch, An introduction to the Kalman filter, in: Proceedings of SIGGRAPH, Course 8, Los Angeles, California, USA, 2001.
[15] G. Campa, M.R. Napolitano, M.L. Fravolini, Simulation environment for machine vision based aerial refueling for UAVs, IEEE Trans. Aerosp. Electron. Syst. 45 (1) (2009) 138–151.
[16] W.B. Blake, D.R. Gingras, Comparison of predicted and measured formation flight interference effect, J. Aircr. 41 (2) (2001) 201–207.
[17] D.R. Gingras, J.L. Player, W.B. Blake, Static and dynamic wind tunnel testing of air vehicles in close proximity, in: Proceedings of AIAA Atmospheric Flight Mechanics Conference, Montreal, Canada, 2001, pp. 2001–4137, AIAA Paper.
[18] J.M. Kelsey, J. Byrne, M. Cosgrove, S. Seereeram, R.K. Mehra, Vision-based relative pose estimation for autonomous rendezvous and docking, in: 2006 IEEE Aerospace Conference, Big Sky, Montana, USA, 2006, pp. 1–20.
[19] P. Wu, J. Lai, J. Wu, S. Chien, Stable pose estimation with a motion model in real-time application, in: 2012 IEEE International Conference on Multimedia and Expo, Melbourne, Australia, 2012, pp. 314–319.
[20] G. Schweighofer, A. Pinz, Robust pose estimation from a planar target, IEEE Trans. Pattern Anal. Machine Intell. 28 (12) (2006) 2024–2030.
[21] R.M. Haralick, H. Joo, C. Lee, X. Zhuang, M.B. Kim, Pose estimation from corresponding point data, IEEE Trans. Syst. Man Cybern. 19 (6) (1989) 1426–1446.
[22] L. Armesto, J. Tomero, SLAM based on Kalman filter for multi-rate fusion of laser and encoder measurements, in: International Conference on Intelligent Robots and Systems, Sendai, Japan, 2004, pp. 1860–1865.